

Phase transitions on Si(113): A high-temperature scanning-tunneling-microscopy study

H. Hibino and T. Ogino

NTT Basic Research Laboratories, Atsugi, Kanagawa 243-01, Japan

(Received 24 February 1997)

Reconstructive phase transitions on Si(113) have been investigated near the critical temperatures using high-temperature scanning tunneling microscopy. During the phase transition between (3×1) and (3×2) reconstructions, (3×2) domains nucleate and fluctuate within the (3×1) domain, and their size increases as the temperature decreases. During the disordering of the (3×1) reconstruction, highly mobile domain walls are observed, which increase in density as the transition is approached from below. The structure and evolution of the domain walls is consistent with disordering of the (3×1) reconstruction via incorporation of $[-]$ (heavy) domain walls. [S0163-1829(97)05231-4]

Whether a (3×2) or (3×1) reconstruction appears on a clean Si(113) surface depends on the temperature.^{1,2} The (3×2) reconstruction is stable at room temperature and experiences a transition to the (3×1) reconstruction. It has been reported that low-energy electron diffraction (LEED) spots related to the (3×2) reconstruction completely disappear at about 500 °C.² The (3×1) reconstruction is also transformed into a (1×1) disordered phase at higher temperatures; the reported disordering temperatures are 570–750 °C.^{2–6} Recently, much effort has been focused on understanding the disordering of the (3×1) reconstruction on a Si(113) surface, and LEED and x-ray-diffraction studies have shown that the disordering belongs to the chiral melting universality class.^{2,4–8} However, little is known about the nature of the (3×2) -to- (3×1) phase transition.

Figure 1 schematically illustrates a (3×1) -reconstructed Si(113) surface including domain walls running normal to the $3\times$ direction along the $[3\bar{3}2]$ direction. There are two types of domain walls, $A|B$ and $B|A$, and they are topologically different. Huse and Fisher called them $[+]$ and $[-]$ domain walls,⁸ whose widths are $(3n+1)a_0$ and $(3n+2)a_0$ ($n=0,1,\dots$), respectively, where a_0 is a unit length along $[1\bar{1}0]$. Conventionally, the two types of walls are referred to as light and heavy because the density of the elements constituting the (3×1) periodicity is lower in the $4a_0$ wide $[+]$ wall and higher in the $2a_0$ wide $[-]$ wall. Chiral melting occurs through the preferred generation of the domain walls with lower energy. Shifts in the positions of the (3×1) diffraction spots have shown that $[-]$ walls are incorporated during the disordering of the (3×1) reconstruction.^{2,6} Recently, Tromp, Theis, and Bartelt investigated critical fluctuations during the disordering of the (3×1) reconstruction in real space and real time using low-energy electron microscopy (LEEM) and showed an increased spatial correlation near the phase-transition temperature and the associated slowing down of the relaxation of long-wavelength critical fluctuations.⁹ This LEEM study greatly contributed to understanding the general critical behavior of continuous phase transitions. However, because the spatial resolution of LEEM was 40 nm and the image contrast originated from the difference in the work function between the ordered and disordered phases,⁹ the incorporation of domain walls, which is

a key to understanding the nature of the disordering of the (3×1) reconstruction, was not observed.

In this paper, we investigate the reconstructive phase transitions on Si(113) on an atomic scale using high-temperature (HT) scanning tunneling microscopy (STM). In HT-STM images of the (3×1) -to- (3×2) phase transition, local (3×2) orders appear in a large (3×1) domain. HT-STM images of the disordering of the (3×1) reconstruction confirm that the disordering occurs through the incorporation of the domain walls.

We observed phase transitions on Si(113) in real space using a commercial scanning tunneling microscope (JEOL JSTM4500 VT), which enables us to observe surface atomic structures at elevated temperatures. The base pressure of the chamber was 3×10^{-8} Pa, and the pressure during HT-STM measurements was below 1×10^{-7} Pa. The Si(113) samples (P-doped, 1–10 Ω cm) were cleaned by repeated oxidation in $\text{H}_2\text{SO}_4\text{H}_2\text{O}_2=1:4$ and oxide removal in HF solution, and protective oxide layers were formed as the final step. They were introduced into UHV through a load lock. The samples were outgassed at about 600 °C for several hours, and then cleaned by flashing at 1250 °C. They were annealed by passing electric currents through them. The sample temperatures below 600 °C were estimated by extrapolating the relation between the heating current and the temperature measured above 600 °C with an infrared pyrometer. The uncertainty of the temperature below 600 °C is probably less than ± 50 °C. STM images were taken in the constant current mode.

Figure 2 shows STM images of (3×2) - and (3×1) -reconstructed Si(113) surfaces. Figures 2(a) and 2(b) were taken at room temperature and 663 °C, respectively. The insets show Fourier transforms (FT) of the images. Unit cells of the (3×2) and (3×1) reconstructions are also indicated in these images. In the STM image of the (3×1) reconstruction, bright spots are arranged in a (3×1) symmetry. The striped contrasts seen in each bright spot are artifacts due to mechanical vibrations. We normally observed no domain walls of the (3×1) reconstruction in 50×50 nm² STM images. Therefore, sharp spots originating from the reconstruction appear in the FT. On the other hand, in large-scale STM images of the (3×2) reconstruction taken at negative sample biases, every other row of features along $[1\bar{1}0]$ looks almost continuous, which corresponds to the $\times 2$ symmetry. As has

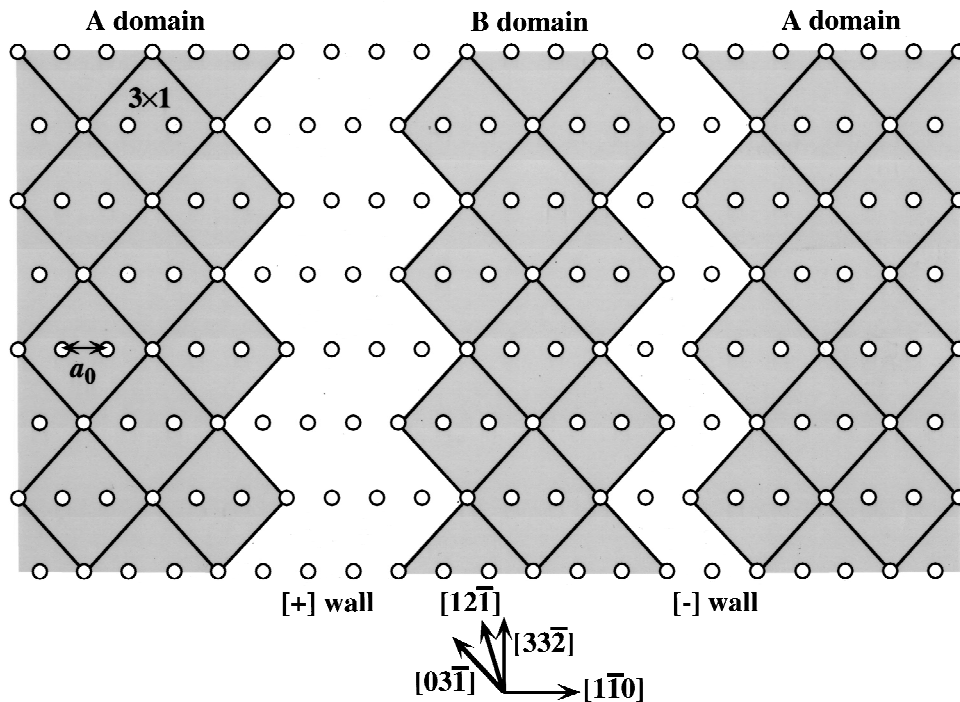


FIG. 1. Schematic illustration of the (3×1) reconstruction on Si(113). Squares show unit cells of the (3×1) reconstruction. Two types of domain walls between A and B domains are shown. A|B and B|A domains are called $[+]$ and $[-]$ walls, respectively.

been already reported, the (3×2) surface consists of small domains, but the $3 \times$ symmetry is continuous across the domain walls.¹⁰ Therefore, in the FT, spots related to the (3×1) symmetry remain sharp, but spots associated with only the (3×2) symmetry are broad.

The bulk-terminated Si(113) surface consists of alternating (111) and (001) terraces, which are both single-atomic-row wide in the $[33\bar{2}]$ direction. Ranke first proposed four structure models for Si(113).¹ Ranke's dimerized model for the (3×1) reconstruction is supported experimentally,¹¹ and recent *ab initio* calculations show that this model is locally stable in terms of surface free energy.¹² The (3×1) dimerized model is essentially based on rebonding at (001) steps and dimer formation on (001) terraces. Recently, Dabrowski, Müssig, and Wolff proposed a model for the (3×2) reconstruction employing the idea of the self-interstitial.¹² Ranke's (3×1) dimerized model has two pentagons, each of which involves a dimer in a (3×2) unit cell. In the (3×2) model of Dabrowski, Müssig, and Wolff, a Si self-interstitial atom is

inserted into one of the two pentagons.¹² The model of Dabrowski, Müssig, and Wolff for the (3×2) reconstruction well reproduces the observed STM images.^{12,13} In the simulated STM image of the (3×2) model of Dabrowski, Müssig, and Wolff at the sample bias of -2 V, rebonded atoms and dimers in the pentagons without interstitials look bright,¹² which agrees with our result that every other row of bright features along $[1\bar{1}0]$ looks almost continuous [Fig. 1(a)]. Dabrowski, Müssig, and Wolff also showed that the surface free energy for a (3×1) model, in which all pentagons include self-interstitials, is equal to that for Ranke's (3×1) dimerized model.¹² Furthermore, Sakama *et al.* recently investigated the structures of defects on the (3×2) surface, one of which was found to basically correspond to the (3×1) symmetry.¹³ They showed that the STM image of this defect is well explained by introducing a Si interstitial atom into the pentagon at the defect site.¹³ These reports suggest that the transition between (3×1) and (3×2) reconstructions may be explained by simple addition or extraction of interstitial

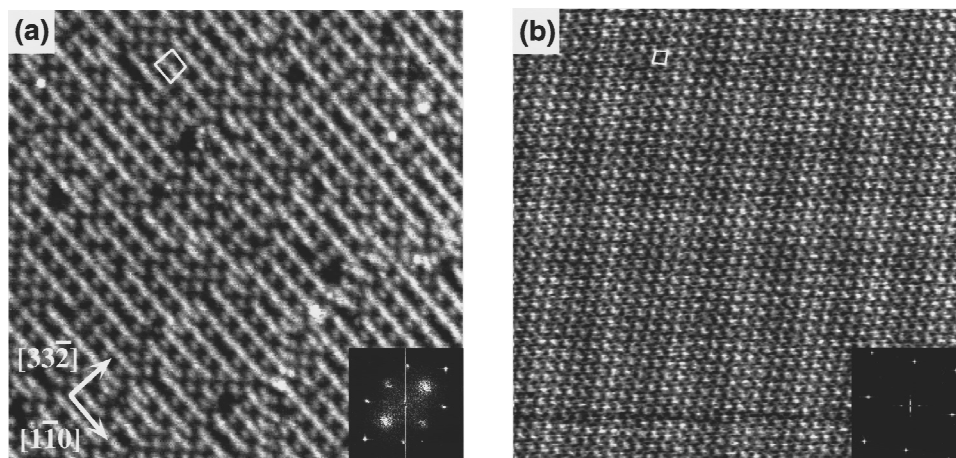


FIG. 2. STM images of Si(113) surfaces taken at (a) room temperature and (b) 663 °C. Insets show their Fourier transforms. The sample biases were -2 and -1.2 V. The tunneling currents of (a) and (b) were 0.1 and 0.07 nA, respectively. The image area is 30×30 nm².

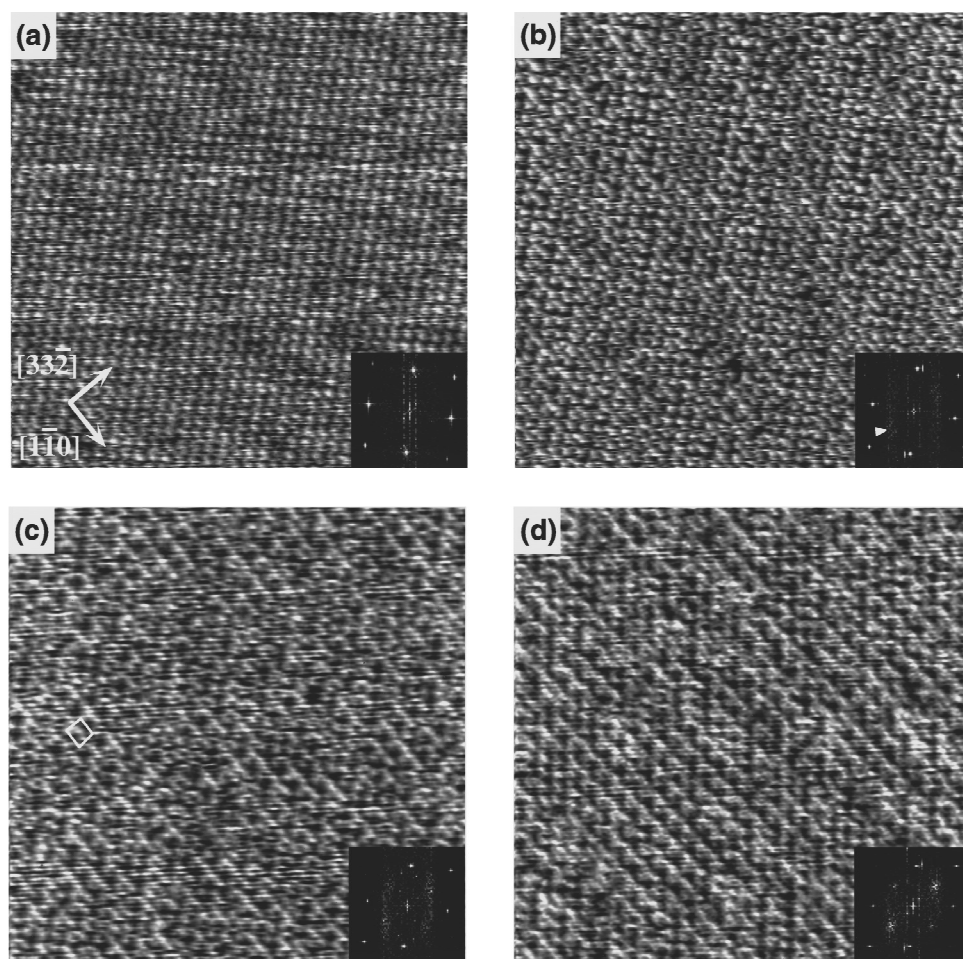


FIG. 3. STM images of Si(113) surfaces taken at (a) 415 °C, (b) 375 °C, (c) 340 °C, and (d) 295 °C. Insets show their Fourier transforms. The sample biases of (a), (b), (c), and (d) were -1 , -2.1 , -2.1 , and -2.4 V, respectively. The tunneling currents were 0.07, 0.1, 0.08, and 0.08 nA. The image area is 30×30 nm².

atoms.¹² Later, we will show filled-state HT-STM images showing fluctuations of bright features during the disordering of the (3×1) reconstruction. Here, one should note that, even though only the rebonded atoms appear in these HT-STM images, there are also pentagons with interstitial atoms between the rebonded atoms. The motion of the rebonded atoms thus should be accompanied by the motion of the pentagons.

Figure 3 shows HT-STM images taken at various temperatures near the (3×2) -to- (3×1) phase transition. The insets show the FT's of the images. The STM image taken at 415 °C [Fig. 3(a)] shows the (3×1) reconstruction with long-range order similar to that of Fig. 2(b) taken at 663 °C. In the STM image taken at 375 °C, however, some bright features have lengthened and connected along $[1\bar{1}0]$. In the model of Dabrowski, Müssig, and Wolff, this indicates that some interstitial atoms have left pentagons. At 375 °C, $\times 2$ order starts to appear locally, resulting in diffuse $\times 2$ spots in the FT, as indicated by the arrow head. In the STM image taken at 340 °C [Fig. 3(c)], (3×2) units can be clearly seen, as indicated by the square, and (3×2) domains are localized. In the STM image taken at 295 °C [Fig. 3(d)], the domain size has increased and the (3×2) domains almost come in contact with each other. The FT's show that the $\times 2$ peaks intensify and sharpen as the temperature decreases. These HT-STM images show that many (3×2) domains nucleate in a (3×1) domain, and that the (3×2) domain size increases until the (3×2) domains cover the surface as the temperature de-

creases. The LEED results of the (3×2) -to- (3×1) transition showed that the (3×2) spots completely disappear at about 500 °C.² This temperature is higher than that at which a $\times 2$ order starts to appear in HT-STM images. The difference is probably because the slow time resolution of STM prevents small domains, which appear and disappear at a fast rate, from being imaged and the dynamic range of the LEED intensity is much wider than that of the FT's of the STM images, which is partly due to the limited scanning area of STM.

Figure 4 shows sequential HT-STM images of the Si(113) surface at 295 °C taken with a 12-s time interval. These surfaces consist of two types of (3×2) domains *A* and *B*, which are different with respect to the $\times 2$ symmetry. In Fig. 4, domain walls are indicated by solid lines. Comparison between these HT-STM images indicates that the domain walls shift in the directions indicated by the arrows. One can also see that a *B* domain nucleates in an *A* domain. These results indicate that the (3×2) surface is divided into fluctuating small domains under thermal equilibrium. The width of the (3×2) domain is at most 10 nm at 295 °C.

Next, we show results on the disordering of the (3×1) reconstruction. Figure 5 shows HT-STM images taken at 663–680 °C. The insets show the FT's. The HT-STM image at 663 °C [Fig. 5(a)] shows a single domain of the (3×1) reconstruction. At 663 °C, no domain walls were typically observed in 50×50 nm² HT-STM images. However, in the HT-STM image taken at 673 °C [Fig. 5(b)], there are some

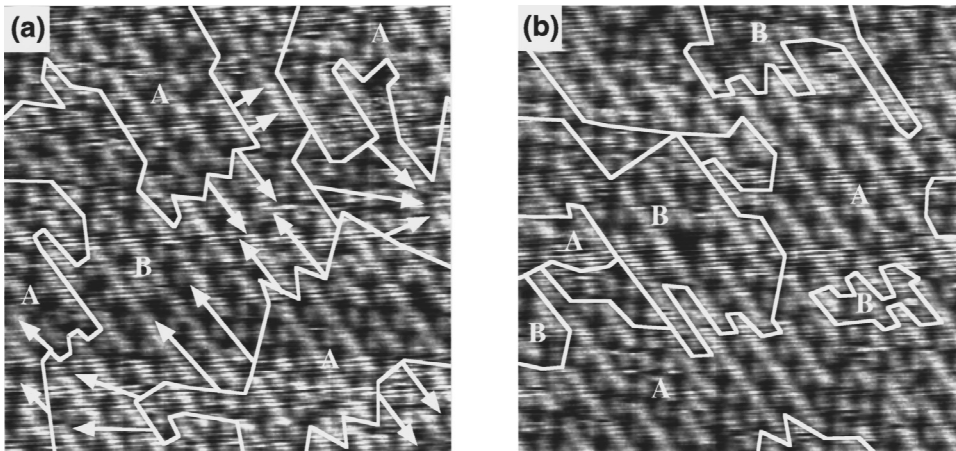


FIG. 4. Sequential STM images of Si(113) surfaces taken at 295 °C. The sample bias and tunneling current were -1.88 V and 0.08 nA, respectively. The image area is 18×18 nm².

fluctuations of the features in the (3×1) reconstruction. However, the features are still arranged on straight lines along $[1\bar{1}0]$. This indicates that the fluctuations are not caused by extrinsic factors such as fluctuations of the temperature, fluctuations of the heating voltage, and mechanical vibrations, but that they are intrinsic. In the (3×1) reconstruction, troughs along $[03\bar{1}]$ are straight, as indicated by a straight line in Fig. 5(a). However, in Fig. 5(b), troughs along $[03\bar{1}]$ are not continuous, but are shifted several times. Thus, the image shown in Fig. 5(b) is divided into several (3×1) domains. The (3×1) spots in its FT are therefore more diffuse than those in Fig. 5(a). However, we must consider

the temporal effect of STM scanning to interpret the apparent domain walls. Horizontal rastering made this STM image, and it took 17.5 s to make. The apparent domain walls are almost parallel to the scanning direction. However, this does not necessarily mean that real domain walls favor this crystallographic direction, since apparent walls were normally seen along the scanning direction even after changing it. We thus conclude that, at 673 °C, the domain walls fluctuate over a width comparable to the scanning area (50 nm) at a speed comparable to the scanning speed (2900 nm/s). Thus, apparent domain walls are seen along the scanning direction in the STM images as the real domain wall fluctuates back

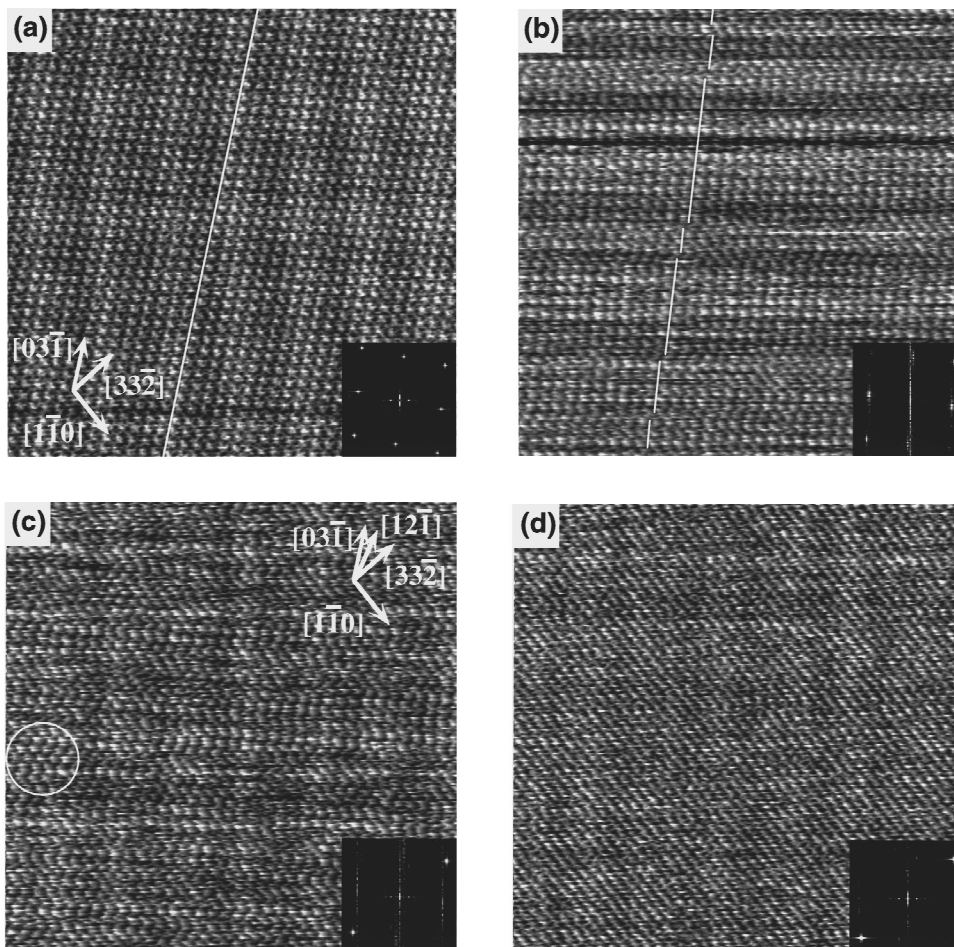


FIG. 5. STM images of Si(113) surfaces taken at (a) 663 °C, (b) 673 °C, (c) 675 °C, and (d) 680 °C. Insets show their Fourier transforms. The sample biases of (a), (b), (c), and (d) were -1.2 , -1 , -0.8 , and -0.8 V, respectively. The tunneling current was 0.07 nA. The image area is 30×30 nm².

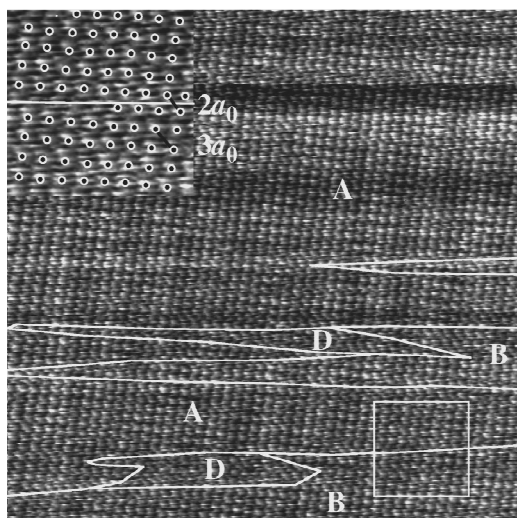


FIG. 6. STM image of a Si(113) surface including a domain wall taken at 670 °C. The nominal domain walls are indicated by solid lines, and the types of the domains are also indicated. The sample bias and tunneling current were -1.3 V and 0.06 nA, respectively. The image area is 44×44 nm². The inset is a magnified STM image of the area indicated by the square. In the inset, bright features are indicated by circles.

and forth across the scan line.

As the temperature is further increased to 675 °C [Fig. 5(c)], fluctuations in the (3×1) reconstruction get larger. In this image, it looks as if the troughs along $[03\bar{1}]$ meander. The apparent domain walls thus are no longer restricted to the scan direction. Regions in which bright features are arranged in a (3×1) symmetry are localized in a few (3×1) units normal to the scanning direction. Therefore, the FT includes (3×1) peaks that are greatly broadened normal to the scanning direction. In the STM image at 680 °C [Fig. 5(d)], the $3 \times$ symmetry disappears, consistent with the disappearance of (3×1) peaks in the FT. This image only shows that bright lines along $[\bar{1}10]$ are arranged in a $1 \times$ symmetry. The lines look almost continuous, and the $1 \times$ spacing cannot be seen in the lines. This may indicate that the features seen in the STM images of the (3×1) reconstruction move along the $[\bar{1}10]$ direction. These HT-STM results clearly show the incorporation of domain walls during the disordering of the (3×1) reconstruction and the increasing density of the domain walls as the temperature increases.

Diffraction studies have shown that the disordering of the (3×1) reconstruction occurs through the incorporation of the $[-]$ wall.⁶ We, therefore, tried to verify this using HT-STM. Figure 6 shows a HT-STM image at 670 °C including apparent domain walls. In this image, the apparent domain walls are indicated by solid lines, and two types of domains are

indicated by *A* and *B*. The regions marked *D* are regions in which fluctuations of bright features are too severe for us to identify the types of domains. The pattern of the apparent domain walls probably indicates that the surface shown in this image is divided into *A* and *B* domains (respectively located in the upper and lower regions of the image) by a widely meandering domain wall running from the middle right to lower left. It is possible to identify the structure of the real domain wall by measuring the displacement across the apparent domain wall as in the area indicated by the square. A magnified view of this area is shown as an inset. The upper and lower halves of the image correspond to *A* and *B* domains. In this figure, the positions of the features are indicated by circles. This image clearly shows that the distance between the features across the domain wall is $2a_0$. This indicates that this domain wall is the $[-]$ one, which seems to agree with the diffraction results that the disordering of the (3×1) reconstruction is accompanied with the incorporation of the $[-]$ walls. However, we cannot assert that all the domain walls seen in the STM images are $[-]$ domain walls. This is due to large fluctuations of the bright features around the domain wall, which makes the structures of the domain boundary unclear, and the slow time resolution of STM, which causes the domain walls seen in the STM images to be apparent walls. However, we have found other evidence of the incorporation of the $[-]$ wall. In the HT-STM image taken at 675 °C [Fig. 5(c)], the troughs, which should be along $[03\bar{1}]$ in the (3×1) reconstruction, are rotated from $[03\bar{1}]$ in some regions, one of which is encircled. In these regions, the troughs are almost along $[\bar{1}2\bar{1}]$ and the distance between the features in the $[\bar{1}10]$ direction are nearly $2a_0$. We suggest that bunches of $[-]$ walls $2a_0$ in width, which correspond to the heavy wall, are formed near the disordering transition, and that they are imaged by STM because they move more slowly than an individual domain wall. The formation of the bunches of the $[-]$ walls further indicates that the $[-]$ walls are incorporated during the disordering of the (3×1) reconstruction.

In summary, we have investigated the reconstructive phase transitions on Si(113) using HT-STM. During the (3×1) -to- (3×2) phase transition, (3×2) domains nucleate in a large (3×1) domain, and their size increases as the temperature decreases. The HT-STM images have also shown that the disordering of the (3×1) reconstruction occurs through the incorporation of domain walls. We observed bunches of $[-]$ walls near the disordering transition, which is consistent with incorporation of $[-]$ walls during the disordering of the (3×1) reconstruction.

We would like to thank Professor Ellen D. Williams for helpful discussions.

¹W. Ranke, Phys. Rev. B **41**, 5243 (1990).

²J. Schreiner, K. Jacobi, and W. Selke, Phys. Rev. B **49**, 2706 (1994).

³B. Z. Olshanetsky and V. I. Mashanov, Surf. Sci. **111**, 414 (1981).

⁴Y.-N. Yang, E. D. Williams, R. L. Park, N. C. Bartelt, and T. L.

Einstein, Phys. Rev. Lett. **64**, 2410 (1990).

⁵D. L. Abernathy, R. J. Birgeneau, K. I. Blum, and S. G. J. Mochrie, Phys. Rev. Lett. **71**, 750 (1993).

⁶D. L. Abernathy, S. Song, K. I. Blum, R. J. Birgeneau, and S. G. J. Mochrie, Phys. Rev. B **49**, 2691 (1994).

⁷D. A. Huse and M. E. Fisher, Phys. Rev. B **29**, 239 (1984).

- ⁸D. A. Huse and M. E. Fisher, *Phys. Rev. Lett.* **49**, 793 (1982).
- ⁹R. M. Tromp, W. Theis, and N. C. Bartelt, *Phys. Rev. Lett.* **77**, 2522 (1996).
- ¹⁰J. Knall, J. B. Pethica, J. D. Todd, and J. H. Wilson, *Phys. Rev. Lett.* **66**, 1733 (1991).
- ¹¹K. Jacobi and U. Myler, *Surf. Sci.* **284**, 223 (1993).
- ¹²J. Dabrowski, H.-J. Müssig, and G. Wolff, *Phys. Rev. Lett.* **73**, 1660 (1994).
- ¹³H. Sakama, D. Kunimatsu, M. Kageshima, and A. Kawazu, *Phys. Rev. B* **53**, 6927 (1996).